Review Article

Abbane Sara, Boussaid Mohammed*, and Dib Anis Sami Amine

Examination of the gamma radiation shielding properties of different clay and sand materials in the Adrar region

https://doi.org/10.1515/phys-2025-0156
received January 25, 2025; accepted April 15, 2025

Abstract: Four samples of natural sand and clay materials from the Adrar region in southern Algeria were studied for their shielding parameters at three chosen energies in this work (0.662, 1.172,1.333 MeV). There was only a small difference between the outcomes demonstrated by Géant 4 and WinXcom. Due to the nearly equal density of the materials examined, the shielding coefficients were likewise similar. But the green clay was the best, as the value of the linear attenuation coefficient (LAC) is equal to 0.117 cm^{-1} at photon energy was 1.172 MeV and it required a small thickness half-value layer equal to 5.903 cm. Subsequently, sand, red clay, and white clay follow green clay in a sequential manner.

Keywords: clay, attenuation coefficient, WinXCom program, Geant 4

1 Introduction

The wide range of uses of ionizing radiation is in nuclear research centers, in health and medical physics, in industries, and even in the agricultural field. This prompts us to take caution in dealing with radiation and enhance protection, especially in buildings and facilities where radiation is present. It must have high shielding ability [1–4].

*** Corresponding author: Boussaid Mohammed**, Energy, Environment and Information Systems Laboratory, Department of Material Sciences, University of Ahmed Draia Adrar, Adrar, Algeria, e-mail: moh.boussaid@univ-adrar.edu.dz
Abbane Sara: Energy, Environment and Information Systems Laboratory, Department of Material Sciences, University of Ahmed Draia Adrar, Adrar, Algeria, e-mail: sa.abbane@univ-adrar.edu.dz
Dib Anis Sami Amine: Radiation Analysis and Application Laboratory, University of Science an Technology of Oran, Oran, Algeria, e-mail: anis.dib@univ-usto.dz

We investigate the attenuation coefficient of the materials, which is the total of the attenuation coefficients of the interactions that occur with the photon (photoelectric interaction, Compton scattering, binary creation), to acquire an adequate shielding capacity. The attenuation coefficient of a substance is related to the photon energy, atomic number, and density of the substance [5–13].

Because of this, lead and concrete are among the most frequently utilized materials and have proven high shielding performance in several studies and research projects. Nevertheless, because it is costly to create big buildings and toxic to the environment, it still has a negative effect [14].

This is the reason behind research efforts to create and enhance shielding coefficients for safe and environmentally friendly materials. For example, despite having low chemical properties and being susceptible to weather and climate, the mixture of sand and clay used in ancient buildings has a high melting point, indicating that it will remain thermally stable when exposed to radiation over a long period of time [15,16].

According to the research [17] on four clay samples collected from various locations in Egypt and compared to ordinary concrete, it has a shielding capacity comparable to other commonly used radiation shields.

Researchers [16] conducted a study on four different types of clay from different parts of Nigeria. They compared the attenuation coefficients of clay materials were measured for gamma photon energies ranging from 100 to 2,000, using known shielding materials such as iron and concrete. They found that spherical clay is superior to ordinary concrete at low photon energies and extremely similar at high photon energies.

The attenuation coefficient values can be calculated using the WinXcom software, which has demonstrated results in numerous research that are closely comparable to the theoretical results [18]. However, when the software's results are compared to those of the Genat4 simulator, they are extremely accurate and nearly match the experimental results [19].

Our current investigation uses both WinXcom and Genat4 simulators to discuss the attenuation coefficients and shielding

properties of clay materials found in southern Algeria. It then compares these findings to studies from Egypt and Nigeria as well as other common shielding materials.

2 Theory

If a photon beam of intensity I goes through a barrier with thickness x, it interacts with matter atoms through a variety of processes. Scattering, absorption, and path change are some of these interactions. This is shown by the attenuation coefficient [20], which can be calculated using the equation below:

$$\frac{\mathrm{d}I}{\mathrm{d}x} = \mu I, \tag{1}$$

$$I = I_0 \exp(-\mu x). \tag{2}$$

The total attenuation coefficient (μ or μ_{total}) for a specific gamma radiation energy is determined by adding together the attenuation coefficients for photoelectric absorption, Compton scattering, and any other significant mechanisms [21]

$$\mu_{\text{total}} = \mu_{\text{photo}} + \mu_{\text{compton}} + \mu_{\text{pair-production}}. \tag{3}$$

The attenuation coefficient in conjunction with the material's density can be used to determine the quantity of gamma radiation that passes through a certain thickness of shielding material. The following equation allows us to express the attenuation coefficient in terms of the mass attenuation coefficient [5]:

$$\mu = (\mu/\rho)\rho = \mu_s \rho. \tag{4}$$

By substituting this into the Eq. (1), we can write the following:

$$I = I_0 \exp(-\mu_s d). \tag{5}$$

In linear form, we can write the following:

$$\ln I = -\mu_s d + \ln I_0. \tag{6}$$

The mass attenuation coefficient of a compound or mixture is equal to the sum of the individual contributions of all the constituent parts. Therefore, according to the mixture rule, we write the following:

$$\mu_s = \left(\frac{\mu}{\rho}\right)_{\text{mix}} = \sum_i \omega_i \left(\frac{\mu}{\rho}\right)_i, \tag{7}$$

where ω_i is the proportion by weight.

A material's thickness that is necessary to attenuate radiation to half its initial intensity (50%) is referred to as half-value layer (HVL) [22]. It can be calculated as follows:

$$\text{HVL} = \frac{\ln 2}{\mu}. \tag{8}$$

The term tenth value layer (TVL) refers to the thickness of material needed to attenuate radiation to 90% of its initial intensity, and it can be calculated as follows [22]:

$$\text{TVL} = \frac{\ln 10}{\mu}. \tag{9}$$

Mean free path (MFP) refers to the thickness of the material needed to attenuate radiation to 63.2% of its initial

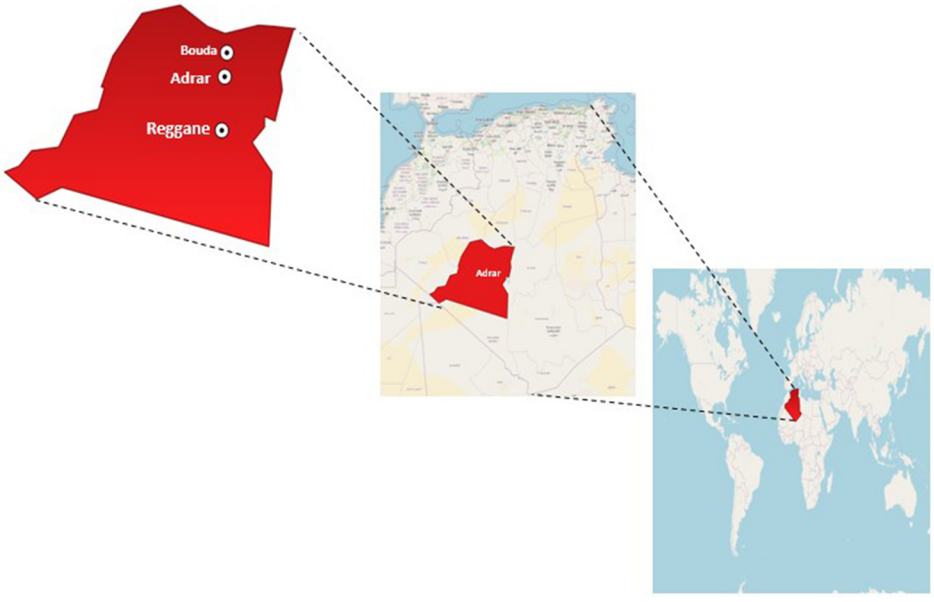

Figure 1: An image depicting the specific locations from where samples were collected.

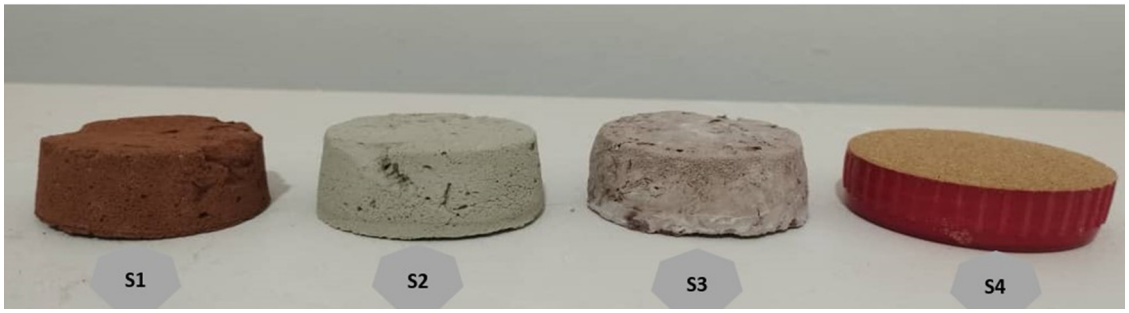

Figure 2: Photos showing the studied samples) S1 = red clay, S2 = green clay, S3 = white clay, S4= sand).

intensity and can be calculated using the following equation [22]:

$$\text{MFP} = \frac{1}{\mu}. \tag{10}$$

3 Materials and methods

3.1 Preparation and analysis of samples

The Adrar region is located 1,500 km south of Algeria and is famous for its traditional construction method using clay and sand [23,24]. Four samples were taken from different locations in the Adrar region; the first region, the Reggane region, which was a field for French nuclear tests [25]. We collected a sample of red clay, some sand, and some green clay from the Adrar region, the center of the state, and some white clay from the Buda region. Figure 1 shows the location of these areas. We use the following symbols to identify the samples: S1 = red clay, S2 = green clay, S3 = white clay, S4 = sand. Figure 2 displays photos of the studied samples. After removing all impurities from each sample, we grind it, let it dry in the sun, and then bake it at a high temperature 100°C [26].

Our scanning electron microscope (SEM) is equipped with an energy-dispersive X-ray spectroscopy (EDX) preprobe for quantitative chemical analysis of samples of interest [27]. To illustrate the particle distribution within each clay type, as shown in Figure 3, and analyze the elemental compositions of these clay types. The compositions are listed in Table 1.

3.2 Calculate the mass attenuation coefficient using WinXCom

WinXCom is an online program that computes photon interaction mass attenuation coefficients (μm) or cross-sections for elements, compounds, and mixtures. The data can be presented as attenuation coefficients (μ), total cross-sections, and partial cross-sections for various processes including incoherent and coherent scatterings, photoelectric absorption, and pair production within the atomic nucleus and electrons. The elemental compositions obtained from EDX of clay samples were utilized. The computation relies on Eqs. (5) and (6) [18].

3.3 Calculate the mass attenuation coefficient using Geant 4

Geant 4 is a widely used toolset for simulating the movement of particles through materials using the Monte Carlo method. The software is based on object-oriented programming and allows users to create classes that define the geometry of the detector, the generator of primary particles, and models of physics processes related to electromagnetic, hadronic, and decay physics. These models can be based on theoretical frameworks, experimental data, or parameterizations. Physics process models usually include various phenomena such as multiple scattering, ionization, Bremsstrahlung, positron annihilation, photoelectric effect, Compton and Rayleigh scattering, pair production, synchrotron and transition radiation, Cherenkov effect, refraction, reflection, absorption, scintillation, fluorescence, and Auger electron emission [28–31]. We also used the elemental compositions obtained from EDX of used clay samples.

4 Results and discussion

4.1 Analysis of elements

Table 1 presents the results of the elemental analysis (SEM/EDX) of the materials under study. The results showed that

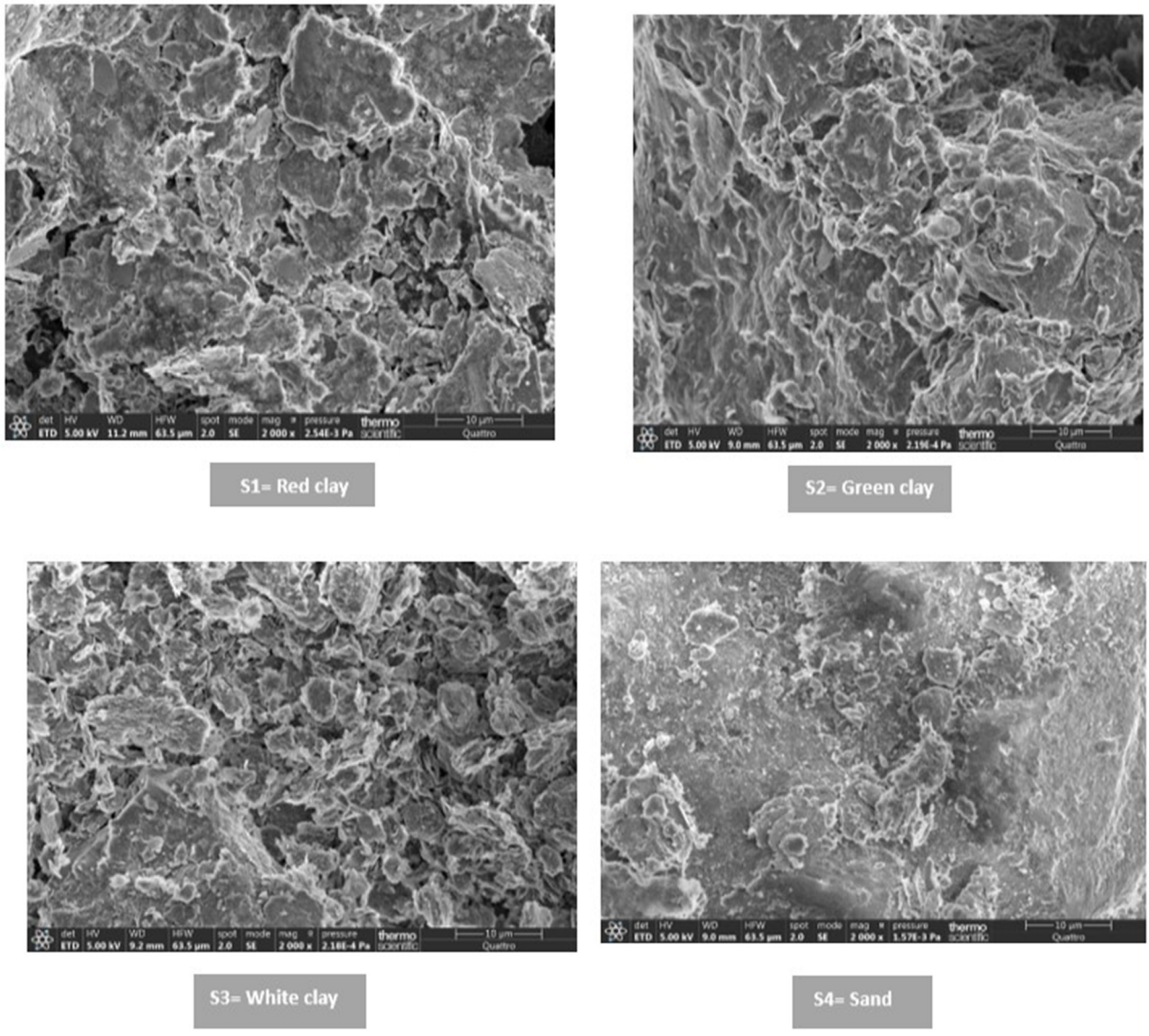

Figure 3: Photos of the studied samples captured with an SEM.

Table 1: Composition of the samples' elements

Element	Sample S1 Density = 1.97 g cm^{-3}	Sample S2 Density = 1.99 g cm^{-3}	Sample S3 Density = 1.98 g cm^{-3}	Sample S4 Density = 1.99 g cm^{-3}
O	58.35	45.69	42.77	53.40
Fe	0.21	1.91	0.71	3.55
Co	0.03	1.10	0.58	0.62
Al	6.70	9.38	18.53	6.48
Si	27.78	28.44	26.44	28.53
K	4.65	7.64	4.85	4.09
Ca	2.29	2.47	0.43	3.33
Mg	—	3.36	—	—
Na	—	—	5.69	—

oxygen is the dominant element in all samples, confirming its position as the most widespread element in the Earth's crust. It was followed by Si, which showed constant percentages in all samples, with a maximum percentage of 28.44 in green clay and a minimum of 26.44 in white clay. The remainder consists of alkali and alkaline earth metals and elements (Fe, Co, Al, Si, K, Ca). The green clay contains Mg at a concentration of 3.36, a characteristic not found in other samples. On the contrary, white clay alone has an Na concentration of 5.69.

SEM/EDX was utilized to demonstrate the distribution of grains [32] in each type of clay: S1 = red clay, S2 = green clay, S3 = white clay, S4 = sand, as depicted in Figure 3. We

observe variations in the morphology and dimensions of the grains among the samples. The particles in A and B were clearly defined and greater in size.

4.2 Calculation of μ_s, μ, HVL, TVL, MFP

Tables 2–6 illustrate the theoretical results for the mass attenuation coefficients, linear attenuation coefficient, HVL, TVL, and MFP, respectively. These results were derived from the XCOM software and the Géant 4 program. The study examines four different varieties of clay with three specific energies (energy released Cs-137 and Co-60).

It is interesting to note that the findings acquired from both XCOM and Géant 4 programs in all tables are highly similar, to the extent of being nearly identical.

According to the data in Table 2, we observe that the mass attenuation coefficients drop as the energy increases. This holds for all four samples (S1, S2, S3, S4). At the minimum energy level of 0.662 MeV, the mass attenuation coefficients were identical in all four samples 0.077 $cm^2\ g^{-1}$, with a minor variation observed at higher energy levels.

Table 3, along with Figure 4, displays the linear attenuation coefficients of the samples and their variations with gamma radiation energy. All samples exhibit nearly identical values at the specified gamma radiation energy. This can be attributed to the fact that the samples possess similar densities and chemical compositions, as explained in Eqs. (1)–(7). Samples S2 and S4, in particular, are enriched with metals and contain the highest proportions of (Si, Ca, Co, Fe). As a consequence, they display higher values of the linear attenuation coefficient, which makes them the most efficient materials for shielding.

By examining Tables 4 and 5, it is clear that the values of the HVL and the TVL show an upward trend with increasing energy levels. The results indicated that a small sample of clay was sufficient to effectively absorb radiation at low energies, while thicker samples are required at higher energy levels. As an illustration, in the given sample S2 with an energy of 0.662 MeV, the length of the HVL is precisely 4.523 cm. The HVL has a length of 6.333 cm when the energy is 1.333 MeV.

Table 2: Mass attenuation coefficients (μ_s) of the samples

Samples	Energy (MeV)	μ_s ($cm^2\ g^{-1}$)	
		XCOM	Geant 4
S1	0.060	0.241	0.240
	0.662	0.077	0.077
	1.172	0.059	0.058
	1.333	0.055	0.055
S2	0.060	0.261	0.261
	0.662	0.077	0.078
	1.172	0.059	0.059
	1.333	0.055	0.055
S3	0.060	0.247	0.247
	0.662	0.077	0.077
	1.172	0.058	0.058
	1.333	0.054	0.055
S4	0.060	0.249	0.251
	0.662	0.077	0.077
	1.172	0.058	0.059
	1.333	0.055	0.056

Table 3: Linear attenuation coefficient (μ) of the samples

Samples	Energy (MeV)	μ (cm^{-1})	
		XCOM	Geant 4
S1	0.060	0.475	0.473
	0.662	0.152	0.155
	1.172	0.115	0.117
	1.333	0.108	0.111
S2	0.060	0.519	0.519
	0.662	0.153	0.155
	1.172	0.117	0.117
	1.333	0.109	0.109
S3	0.060	0.489	0.489
	0.662	0.152	0.154
	1.172	0.114	0.116
	1.333	0.106	0.110
S4	0.060	0.496	0.499
	0.662	0.153	0.153
	1.172	0.115	0.117
	1.333	0.109	0.111

Table 4: HVL of the samples

Samples	Energy (MeV)	HVL (cm)	
		XCOM	Geant 4
S1	0.662	4.560	4.471
	1.172	5.975	5.924
	1.333	6.418	6.245
S2	0.662	4.523	4.472
	1.172	5.903	5.924
	1.333	6.333	6.359
S3	0.662	4.560	4.501
	1.172	6.080	5.975
	1.333	6.539	6.301
S4	0.662	4.523	4.530
	1.172	6.005	5.924
	1.333	6.333	6.245

Table 5: TVL of the samples

Samples	Energy (MeV)	TVL (cm)	
		XCOM	Geant 4
S1	0.662	15.146	14.855
	1.172	19.849	19.680
	1.333	21.320	20.744
S2	0.662	15.026	14.855
	1.172	19.611	19.680
	1.333	21.037	21.125
S3	0.662	15.149	14.951
	1.172	20.198	19.845
	1.333	21.723	20.933
S4	0.662	15.026	15.049
	1.172	19.949	19.680
	1.333	21.037	20.744

Table 6: MFP of the samples

Samples	Energy (MeV)	MFP (cm)	
		XCOM	Geant 4
S1	0.662	6.579	6.452
	1.172	8.621	8.547
	1.333	9.259	9.009
S2	0.662	6.526	6.452
	1.172	8.517	8.547
	1.333	9.136	9.174
S3	0.662	6.579	6.493
	1.172	8.772	8.621
	1.333	9.434	9.091
S4	0.662	6.536	6.461
	1.172	8.664	8.589
	1.333	9.136	9.174

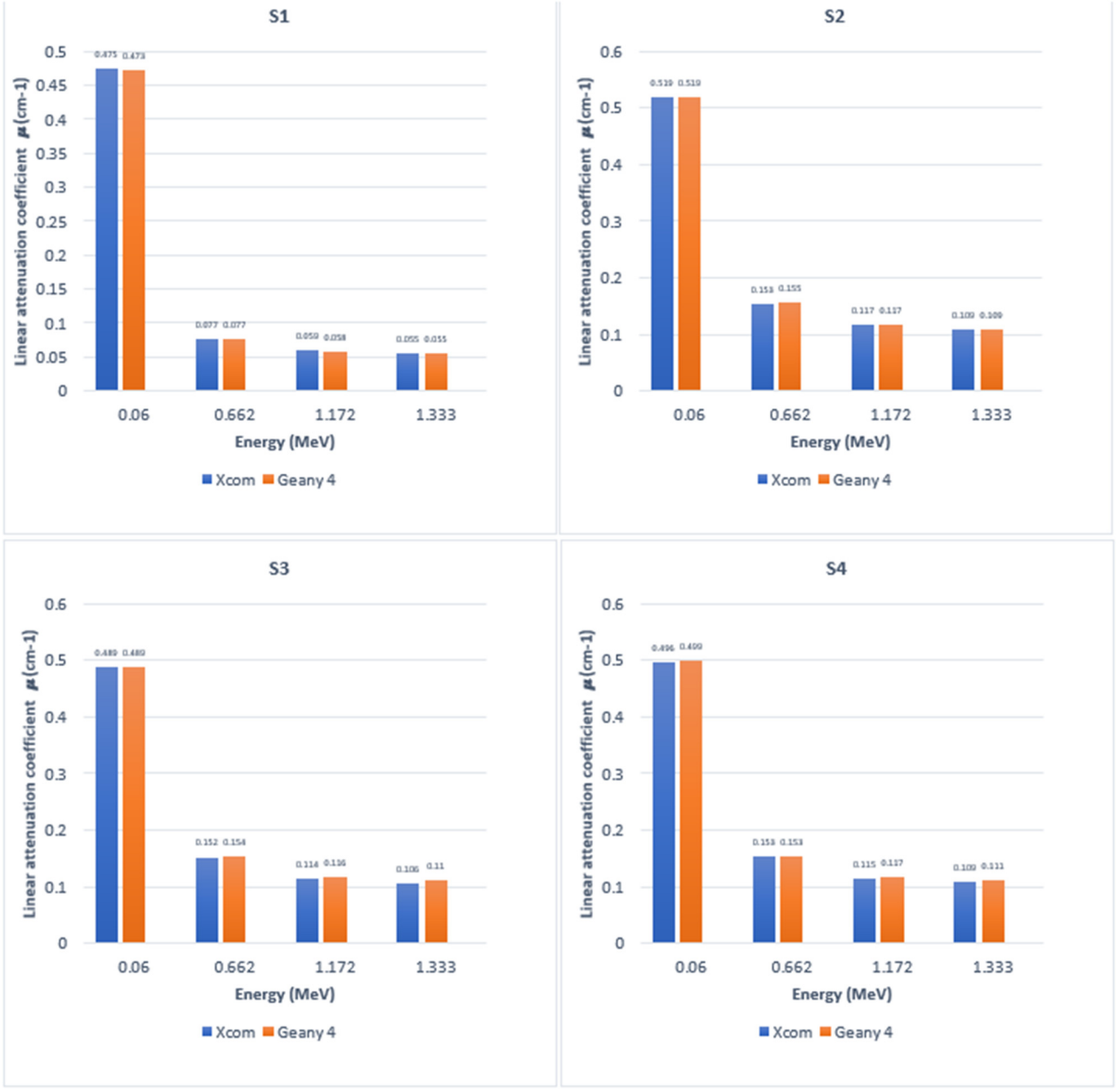

Figure 4: Comparison of linear attenuation coefficient (LAC) values calculated by Geant 4.

Table 7: Shielding parameters of four different clay types were compared to previously published data

Shielding parameters	Energy (MeV)	This work				[16]		[17]	
		S1	S2	S3	S4	Ball clay	Kaolin clay	Bentonite clay	Red clay
LAC	1.172	0.116	0.117	0.114	0.115	0.115	0.115	0.224	0.117
	1.333	0.108	0.109	0.106	0.109	0.108	0.108	0.114	0.110
HVL	1.172	5.975	5.903	6.080	6.005	6.025	6.015	5.664	5.899
	1.333	6.418	6.333	6.539	6.333	6.425	6.413	6.047	6.297
M FP	1.172	8.621	8.517	8.772	8.664	8.694	8.679	8.172	8.510
	1.333	9.259	9.136	9.434	9.136	9.271	9.254	8.725	9.085

In a similar way, according to Table 6, the MFP also increases when the energy of gamma radiation increases. It is observed that the thickness of the material required to attenuate 63.2% of the initial radiation was best in sample S2, followed by S4, S1, and S3.

Table 7 shows the effectiveness of the samples under study [S1, S2, S3, S4] where LAC, HVL, and MFP at high energies 1.172 and 1.333 MeV were compared with previous studies [17,16] of the same nature of clay materials, and their results showed satisfactory values when compared to normal concrete and steel concrete. Upon careful analysis of the table, it is evident that bentonite clay demonstrates superior reading shielding parameters. The greatest LAC value is 0.224 cm^{-1} at a photon energy level of 1.172 MeV and 0.114 cm^{-1} at a photon energy level of 1.333 MeV. The HVL and MFP have the lowest values (5.664, 6.047 cm) and (8.172, 8.725 cm) are read at the energies (1.172, 1.333 MeV), respectively. The green clay sample S2 from our current investigation came next, and it also had good shielding coefficients. At photon energy 1.172 MeV and photon energy 1.333 MeV, the LAC values were equivalent to 0.117 and 0.109 cm^{-1}, respectively. The remaining samples are S4, Ball Clay, Kaolin Clay, and S3, which are in that order.

Table 8 presents a juxtaposition of the experimentally derived MAC values with the WinXCOM results obtained from the study [17]. These results are then compared with the Geant 4 result estimated in this investigation. Upon examining the table, it is evident that the outcomes obtained from Geant 4 were highly consistent with the experimental results across various energy levels and clay kinds. Furthermore, the results from Geant 4 were found to be more closely aligned with the experimental data compared to the results generated by WinXOM, albeit with a minor discrepancy.

Table 8: Shielding parameters of four different clay types were compared to previously published data [17]

Clay type	Energy (MeV)	MAC ($cm^2 g^{-1}$)		
		XCOM	Experimental	Geant 4 (This work)
Red clay	0.06	0.352	0.346	0.351
	0.662	0.076	0.077	0.076
	1.172	0.058	0.056	0.057
	1.333	0.054	0.053	0.054
Ball clay	0.06	0.287	0.282	0.286
	0.662	0.077	0.076	0.076
	1.172	0.058	0.058	0.058
	1.333	0.276	0.270	0.271
Kalion clay	0.06	0.276	0.270	0.274
	0.662	0.077	0.075	0.076
	1.172	0.058	0.059	0.058
	1.333	0.055	0.054	0.054
Bentonite clay	0.06	0.372	0.383	0.379
	0.662	0.077	0.078	0.077
	1.172	0.058	0.057	0.058
	1.333	0.055	0.054	0.054

5 Conclusion

Geant 4 simulation serves as a viable substitute for experimentation when its components are unavailable. Moreover, engaging in pre-experiment work enables the opportunity to meticulously design the experiment and thoroughly analyze all the factors associated with it.

The photoelectric process dominates at low-energy gamma radiation. As the energy increases to a medium level, the Compton interaction process and scattering effect become more prevalent. At high energies, the cogeneration process takes over as the dominant interaction. Materials with high atomic numbers and effective atomic numbers are necessary for this purpose. Consequently, the researched material is particularly useful for low-energy protection. Considering its accessibility, autonomy, and resistance to heat and chemicals, it can be employed in fortified structures for safeguarding purposes.

The investigated samples can be organized in descending order of shielding efficiency as follows: S2, S4, S1, S3.

Funding information: The authors state no funding involved.

Author contributions: All authors have accepted responsibility for the entire content of this manuscript and approved its submission.

Conflict of interest: The authors state no conflict of interest.

Data availability statement: The datasets generated and/or analyzed during the current study are available from the corresponding author on reasonable request.

References

[1] International Atomic Energy Agency (IAEA). Safety standards for protecting people and the environment: Radiation protection and safety in medical uses of ionizing radiation. Vienna: IAEA; 2016.
[2] Abdel Rahman RO, Hung YT. Application of ionizing radiation in wastewater treatment: An overview. Water. 2020;12(1):19. doi: 10.3390/w12010019.
[3] Abdillah M, Qonit H, Indiarto R. A review of irradiation technologies on food and agricultural products. Artic Int J Sci Technol Res. 2020;9(1):4411–4.
[4] Bawazeer O, Makkawi K, Aga ZB, Albakri H, Assiri N, Althagafy K, et al. A review on using nanocomposites as shielding materials against ionizing radiation. J Umm Al-Qura Univ Appl Sci. 2023;9(3):325–40. doi: 10.1007/s43994-023-00042-9, Springer.
[5] Alsayed Z, Badawi MS, Awad R, El-Khatib AM, Thabet AA. Investigation of γ-gamma attenuation coefficients, effective atomic number and electron density for ZnO/HDPE composite. Phys Scr. Aug 2020;95(8):085301. doi: 10.1088/1402-4896/ab9a6e.
[6] More CV, Alsayed Z, Badawi MS, Thabet AA, Pawar PP. Polymeric composite materials for radiation shielding: a review. Environ Chem Lett. 2021;19(3):2057–90. Springer Science and Business Media Deutschland GmbH. doi: 10.1007/s10311-021-01189-9.
[7] Sarihan M. Simulation of gamma-ray shielding properties for materials of medical interest. Open Chem. Jan 2022;20(1):81–7. doi: 10.1515/chem-2021-0118.
[8] Mcalister DR. Gamma ray attenuation properties of common shielding materials. USA: University Lane Lisle; 2012.
[9] Obaid SS, Sayyed MI, Gaikwad DK, Pawar PP. Attenuation coefficients and exposure buildup factor of some rocks for gamma ray shielding applications. Radiat Phys Chem. Jul 2018;148:86–94. doi: 10.1016/j.radphyschem.2018.02.026.
[10] AbuAlRoos NJ, Baharul Amin NA, Zainon R. Conventional and new lead-free radiation shielding materials for radiation protection in nuclear medicine: A review. Radiat Phys Chem. 2019;165:108439. doi: 10.1016/j.radphyschem.2019.108439.
[11] Lakshminarayana G, Elmahroug Y, Kumar A, Dong MG, Lee D-E, Yoon J, et al. Correction to: Li_2O–B_2O_3–Bi_2O_3 glasses: gamma-rays and neutrons attenuation study using ParShield/WinXCOM program and Geant 4 and penelope codes. Appl Phys. 2020;126(5):331. doi: 10.1007/s00339-020-3447-2.
[12] Al-Buriahi MS, Tonguc BT. Mass attenuation coefficients, effective atomic numbers and electron densities of some contrast agents for computed tomography. Radiat Phys Chem. 2020;166:108507. doi: 10.1016/j.radphyschem.2019.108507.
[13] Bantan RAR, Sayyed MI, Mahmoud KA, Al-Hadeethi Y. Application of experimental measurements, Monte Carlo simulation and theoretical calculation to estimate the gamma ray shielding capacity of various natural rocks. Prog Nucl Energy. Aug 2020;126:103405. doi: 10.1016/j.pnucene.2020.103405.
[14] Wani AL, Ara A, Usmani JA. Lead toxicity: A review. Interdiscip Toxicol. 2015;8(2):55–64, Slovak Toxicology Society. doi: 10.1515/intox-2015-0009.
[15] Taqi AH, Khalil HJ. Experimental and theoretical investigation of gamma attenuation of building materials. J Nucl Part Phys. 2017;2017(1):6–13. doi: 10.5923/j.jnpp.20170701.02.
[16] Olukotun SF, Gbenu ST, Ibitoye FI, Oladejo OF, Shittu HO, Fasassi MK, et al. Investigation of gamma radiation shielding capability of two clay materials. Nucl Eng Technol. 2018;50(6):957–62. doi: 10.1016/j.net.2018.05.003.
[17] Elsafi M, Koraim Y, Almurayshid M, Almasoud FI, Sayyed MI, Saleh IH. Investigation of photon radiation attenuation capability of different clay materials. Materials. 2021;14(21):6702. doi: 10.3390/ma14216702.
[18] Gerward L, Guilbert N, Jensen KB, Levring H. WinXCom - A program for calculating X-ray attenuation coefficients. Radiat Phys Chem. 2004;71(3):653–4. doi: 10.1016/j.radphyschem.2004.04.040.
[19] Medhat ME, Singh VP. Mass attenuation coefficients of composite materials by Geant 4, XCOM and experimental data: Comparative study. Radiat Eff Defects Solids. Sep. 2014;169(9):800–7. doi: 10.1080/10420150.2014.950264.
[20] Damla N, Baltas H, Celik A, Kiris E, Cevik U. Calculation of radiation attenuation coefficients, effective atomic numbers and electron densities for some building materials. Radiat Prot Dosimetry. 2012;150(4):541–9. doi: 10.1093/rpd/ncr432.
[21] Fabjan CW, Schopper H. Particle Physics Reference Library Volume 2: Detectors for particles and radiation. Springer Nature; 2020.
[22] Dahinde PS, Dapke GP, Raut SD, Bhosale RR, Pawar PP. Analysis of half value layer (HVL), tenth value layer (TVL) and mean free path (MFP) of some oxides in the energy range OF 122KeV to 1330KeV. Indian J Sci Res. 2019;9(2):79–84. doi: 10.32606/ijsr.v9.i2.00014.
[23] Abdeldjalil M. Determining the characteristics of dune sand used in the building of different sites for the desert environment. 2023. doi: 10.21203/rs.3.rs-3016446/v1.
[24] Abdeldjalil AM. Identification of dune sands used in building by their characteristics and a granular model for an arid environment. Asian J Civ Eng. Apr 2024;25(3):2883–901.
[25] Danesi PR, Moreno J, Makarewicz M, Louvat D. Residual radionuclide concentrations and estimated radiation doses at the former French nuclear weapons test sites in Algeria. Appl Radiat Isotopes. 2008;66(11):1671–4. doi: 10.1016/j.apradiso.2007.08.022.
[26] Mui W, Kuang XM, Zhang H, Bhandari S, Dominguez R, Polidori A, et al. Development of ASTM International D8405—standard test method for evaluating PM2.5 sensors or sensor systems used in indoor applications. J Occup Environ Hyg. 2023;20(9):373–89. doi: 10.1080/15459624.2023.2212739.
[27] Zadora G, Brozek-Mucha Z. SEM-EDX - A useful tool for forensic examinations. Mater Chem Phys. 2003;81(2–3):345–8. doi: 10.1016/S0254-0584(03)00018-X.

[28] Mohamed MO, Dib ASA, Belbachir AH. Energy distribution of cosmic rays in the Earth's atmosphere and avionic area using Monte Carlo codes. Pramana. 2016;87:1–5. doi: 10.1007/s12043-016-1210-1.
[29] Ali Al-zaidi G, Saudi HA, Nassar IA, Sedeek K. Investigation of the radiation Shielding Behavior of Monocrystalline and Polycrystalline solar cell using experimental, Geant 4 Simulation Code and WinXCOM Database. 2023. doi: 10.21203/rs.3.rs-3368703/v1.
[30] de la Fuente Rosales L, Incerti S, Francis Z, Bernal MA. Accounting for radiation-induced indirect damage on DNA with the Geant 4-DNA code. Phys Med. Jul 2018;51:108–16. doi: 10.1016/j.ejmp.2018.06.006.
[31] Belamri C, Dib ASA, Belbachir AH. Monte Carlo simulation of proton therapy using bio-nanomaterials. J Radiother Pract. Sep. 2016;15(3):290–5. doi: 10.1017/S1460396916000145.
[32] Khalaf MA, Ramli M, Ahmed NM, Ahmad MS, Ahmed Ali AM, et al. Modern heavyweight concrete shielding: Principles, industrial applications and future challenges; review. J Build Eng. 2021;39:102290. doi: 10.1016/j.jobe.2021.102290.